Disturbance Observer-Based Control of Tip-Tilt Mirror for Mitigating Telescope Vibrations

Tao Tang, *Member, IEEE*, Shuaixu Niu, Xiaoqiang Chen, and Bo Qi

***Abstract*— In the ground-based astronomical telescope, the imaging quality is usually affected by tip-tilt vibrations induced by the telescope structure. Long exposure time of the image sensor is usually required for a good signal-to-noise ratio, which brings the amount of time delays into the control loop of the tip-tilt mirror. Thus, a low control bandwidth is insufficient to compensate telescope vibrations. In this paper, an improved disturbance observer (DOB) control based on only the image sensor is proposed to reject structural vibrations. This new DOB controller is added into the original loop in the tip-tilt mirror control system, so the closed-loop performance can be optimized by designing an appropriate Q-filter. An improved Q-filter is presented to reject large-magnitude vibrations and also to reduce amplifications induced by this controller at nondisturbance frequencies. This proposed controller can achieve a satisfying result in vibration mitigations when vibration frequencies are provided to design the Q-filter. Furthermore, in the tilt–tilt mirror control system, this improved DOB is not restricted by an accurate model such that noise in the loop cannot provide serious influence on vibration mitigation. Both simulations and extensive experiments are carried out to demonstrate that the DOB can earn an extra improvement on the control performance in comparisons with the conventional feedback controller.**

***Index Terms*— Astronomical telescope, disturbance observer (DOB) control, image sensor, tip-tilt mirror, vibration mitigations.**

I. Introduction

FOR arriving at the optical diffraction limit, mechanical vibrations induced by the telescope structure [1]–[3] have to be mitigated. The optical path length between primary mirrors and the image sensor could be disturbed by structural vibrations [4], [5], which can be caused by transportations, vibration devices, or wind moment [6], [7]. These disturbances caused by a mechanical structure are difficult to be well mitigated by conventional feedback loops [8], [9]. The long integration time of the image sensor (such as charge coupled device) in the astronomical telescope is required to get a high-resolution image for deep-space observations, which produces large time delay to the feedback loop, leading to a restricted closed-loop bandwidth of the tip-tilt mirror control system. Furthermore, many existing large telescopes [10] reveal that the frequency of structure vibrations usually exceeds 5 Hz due to the structural rigidity, while these tip-tilt vibrations feature large amplitude and multiple narrowband [11], which could not be mitigated by a conventional feedback loop, resulting in a limited closed-loop performance. Therefore, structural vibrations have become vital in the astronomical telescope. The new method based on the disturbance feedforward control [12], [13] in the tip-tilt control system to suppress structural vibrations. This controller can produce a high suppression bandwidth because it cannot be limited by a low-rate sampling. However, the accuracy of vibrations estimation is affected greatly by the low-frequency drifts and high-frequency noise of accelerometers or gyroscope [14]. Due to an additional burden brought in an existing control system, many researchers still focus on advanced controllers to reject vibrations. Compared to integral controllers, linear quadratic Gaussian, or H_∞/H_2 controllers [15], [16] are suggested to improve the closed-loop performance under the condition of tip-tilt vibrations. Less than a factor of three or five reductions can be achieved in comparison with the conventional feedback controller [17]. However, the closed-loop performance is dependent on the model accuracy of control plant and the vibration. Especially it could be deteriorated, if large model errors are presented in the tip-tilt mirror control system. The disturbance observer (DOB) [18]–[20] is used to reject disturbance in the low-frequency domain if the disturbance can be estimated or measured accurately, because the disturbance usually occurs in the low-frequency domain, while the sensor noise occurs in the high-frequency domain. In this case, the DOB needs to get a tradeoff between disturbance suppression and control stability. Q_{31}-filter is generally used as an optimal filter in many servo control systems [21]–[23] such that the closed-loop performance can be optimized in terms of control bandwidth and robust stability. If disturbances feature large magnitude in low or medium frequency, the high bandwidth of the low-pass Q-filter is necessary when linear DOB is used in the closed-loop control system. The DOB-based control strategy using backstepping, H_∞ or sliding mode techniques [24], [25] is designed to cope with external disturbance without the high control gain. However, disturbance boundary needs to be known. Furthermore, the closed-loop stability could be carefully considered in these nonlinear DOBs.

In this paper, an improved DOB based on only position error is proposed to mitigate structural vibrations for the astronomical telescope. In the conventional DOB control

Manuscript received June 26, 2018; revised August 20, 2018; accepted August 23, 2018. This work was supported by Youth Innovation Promotion Association, Chinese Academy of Sciences. The Associate Editor coordinating the review process for this paper was Dr. George Xiao. *(Corresponding author: Tao Tang.)*

T. Tang, S. Niu, and B. Qi are with the Institute of Optics and Electronics, Chinese Academy of Sciences, Beijing 100864, China (e-mail: prettang@gmail.com; qibo@ioe.ac.cn or).

X. Chen is with the Institute of Aerospace System Engineering, Shanghai 200108, China (e-mail: cxq1846@163.com).

Color versions of one or more of the figures in this paper are available online at http://ieeexplore.ieee.org.

Digital Object Identifier 10.1109/TIM.2018.2869437

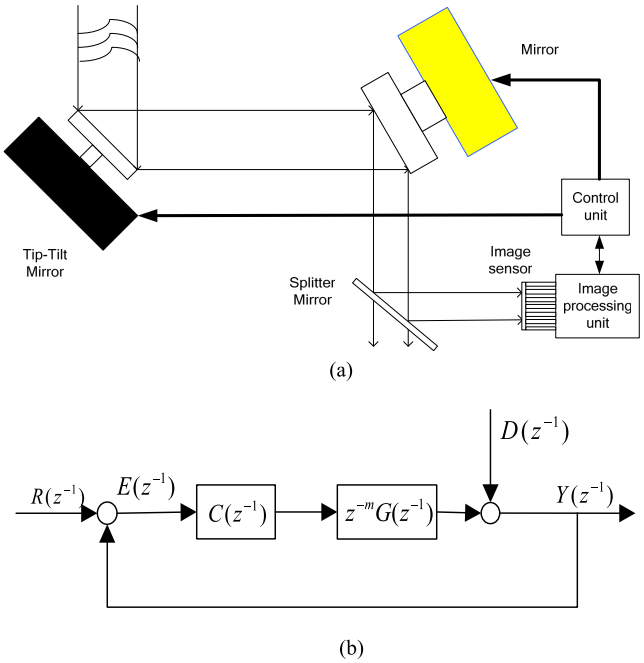

Fig. 1. Schematic of the tip-tilt mirror configuration. (a) Optical path. (b) Classical control structure.

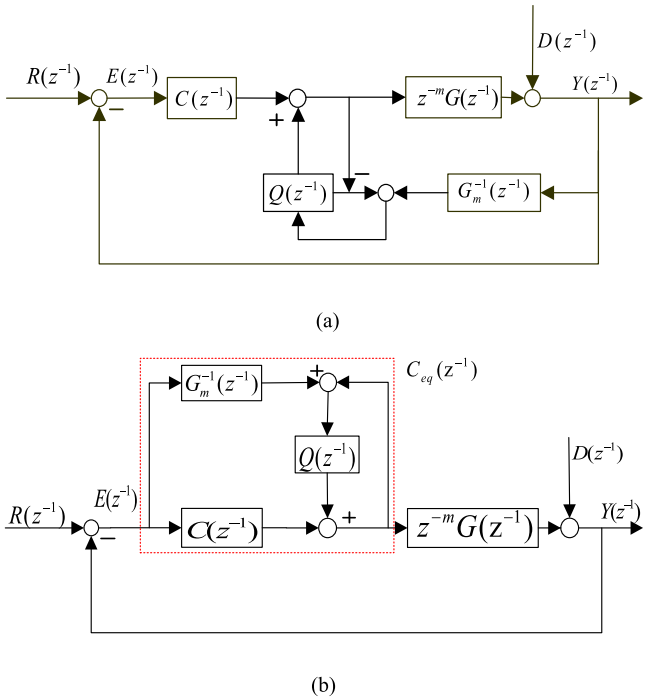

Fig. 2. Schematic of the DOB. (a) Classic DOB structure. (b) Proposed control structure.

system [26], [27], the feedback signal is used to estimate the inverse of the control model. This new DOB controller only uses the error signal and can be added to the current control loop. A modified filter is presented to remove low-frequency oscillations [28]. Motivated by this idea, an enhanced notch filter [29] is developed to cope with multiple narrowband vibrations. Compared with the design method to the Q-filter [30], a new design procedure of the Q-filter in the continuous-time domain is presented because it is very convenient to obtain relations between its parameters and characteristics. The remaining of this paper is arranged in the following. Section II introduces the proposed DOB structure of the tip-tilt mirror, mainly depicting the optical configuration and the control structure of the tip-tilt mirror. The stability and robust stability of this improved DOB control system are discussed in Section III. Section IV gives the design process of the controller and Q-filter parameters. Extensive simulations and experiments are implemented to testify the proposed controller in Section V. Section VI draws a conclusion to this paper.

II. DOB Control of Tip-Tilt Mirror

The brief optical path of the tip-tilt mirror in the astronomical telescope [13] is depicted in Fig. 1(a). Vibrations in the tip-tilt mode can be detected by the image sensor, which provides the line-of-sight errors (position errors) to control the tip-tilt mirror. The conventional control structure of the tip-tilt mirror is demonstrated in Fig. 1(b), which includes only a feedback position loop. The transfer function of $G(z^{-1})$ is a combination of the characteristics of mechanics of the tip-tilt mirror and electronic apparatuses (A/D, D/A, and power drive). $C(z^{-1})$ is the tracking controller. The delay unit z^{-m} represents the time delay in the control system. $R(z^{-1})$ is the control input, and $Y(z^{-1})$ is the output. $E(z^{-1})$ is the closed loop. $D(z^{-1})$ is the disturbance.

The error attenuation function with the integral controller in Fig. 1(b) is expressed as follows:

$$\frac{Y(z^{-1})}{D(z^{-1})} = \frac{1}{1+z^{-m}C(z^{-1})G(z^{-1})}. \tag{1}$$

From (1), it is shown that the closed-loop performance of the tip-tilt mirror control system is dependent on the controller. High controller gain facilitates good corrections. However, the loop bandwidth is mainly restricted by the time delay of the image sensor because the control plant $G(z^{-1})$ usually has more than hundreds of bandwidth. To relax the constraints on time delay, the DOB is brought into the control system. The conventional DOB structure [27] is shown in Fig. 2(a). In the image sensor-based control system, the disturbance $D(z^{-1})$ cannot be directly measured by $Y(z^{-1})$. Therefore, an improved DOB control structure [29], [31] based on only position available is proposed in Fig. 2(b) to reject the disturbance $D(z^{-1})$. $Q(z^{-1})$ is a designed filter, which plays an important role in this DOB system. The inverse of $G(z^{-1})$ is depicted by a nominal model of $G_m^{-1}(z^{-1})$, which can be implemented in a digital control system.

The sensitivity transfer function in Fig. 2(b) when the DOB is used in the control system is expressed in the following equation:

$$\frac{Y(z^{-1})}{D(z^{-1})} = \frac{1-Q(z^{-1})}{1+z^{-m}C(z^{-1})G(z^{-1})+[z^{-m}G(z^{-1})G_m^{-1}(z^{-1})-1]Q(z^{-1})}. \tag{2}$$

In comparison with (1), minimizing $1-Q(z^{-1})$ [called extra sensitivity function ESF(z^{-1})] at the expected frequencies is the objective if $z^{-m}G(z^{-1})G_m^{-1}(z^{-1}) - 1 \approx 0$ in (2).

$$A(z^{-1}) = z^{-m}\frac{G(z^{-1})C(z^{-1}) + Q(z^{-1})G_m^{-1}(z^{-1})G(z^{-1})}{1 + z^{-m}G(z^{-1})C(z^{-1}) + [z^{-m}G_m^{-1}(z^{-1})G(z^{-1}) - 1]Q(z^{-1})} \tag{4}$$

ESF(z^{-1}) is expected to have less than -10 dB or less magnitude response in the interest-frequency domain. Due to an inaccurate model present in $G(z^{-1})$, it is difficult to arrive at $z^{-m}G(z^{-1})G_m^{-1}(z^{-1}-1) = 0$. Thus, $Q(z^{-1})$ has to feature a low-pass filter to suppress the high-frequency dynamics and noise in order to make $[z^{-m}G(z^{-1})G_m^{-1}(z^{-1})-1]Q(z^{-1})$ close to zero. In this case, the closed-loop stability of the control system in Fig. 2(b) can be satisfied. If $Q(z^{-1})$ is a low-pass filter, the smaller the bandwidth of $Q(z^{-1})$ is, the higher is the stability margin. However, the control performance is just the opposite.

III. Stability and Robust Stability Analysis

This section analyzes the stability and robust stability conditions, which provides criterions for the design of the controller parameters. The equivalent controller [31] in the dotted box describing in Fig. 2(b) is expressed in the following equation:

$$C_{\text{eq}}(z^{-1}) = \frac{C(z^{-1}) + G_m^{-1}(z^{-1})Q(z^{-1})}{1 - Q(z^{-1})}. \tag{3}$$

$C_{\text{eq}}(z^{-1})$ is a simplest Youla–Kucrea form [31] if $Q(z^{-1}), G_m(z^{-1})$, and $C(z^{-1})$ are rational and stable. However, it is impossible to implement $G_m(z^{-1}) = G(z^{-1})$ because of high-frequency unmodeled dynamics. Therefore, an enhanced condition is given in the following.

When using the DOB controller, the closed-loop transfer function is derived in (4), as shown at the top of this page.

If $A(z^{-1})$ is stable, its poles are all in the unit circle. It is difficult to solve the result of the characteristics polynomial expressed in the following equation:

$$\begin{aligned} P(z^{-1}) &= 1 + z^{-m}G(z^{-1})C(z^{-1}) + Q(z^{-1}) \\ &\quad \times (z^{-m}G_m^{-1}(z^{-1})G(z^{-1}) - 1) \\ &= (1 + z^{-m}G(z^{-1})C(z^{-1})) \\ &\quad \times \left(1 + \frac{\left(z^{-m}G_m^{-1}(z^{-1})G(z^{-1}) - 1\right)Q(z^{-1})}{1 + z^{-m}G(z^{-1})C(z^{-1})}\right). \end{aligned} \tag{5}$$

Because, the left term $1 + z^{-m}C(z^{-1})G_m(z^{-1})$ of (5) is the original characteristics polynomial and must be stable, according to the small-gain theorem, the stability condition of this DOB control system has to meet in the following equation:

$$\left\| Q(z^{-1})\frac{z^{-m}G_m^{-1}(z^{-1})G(z^{-1}) - 1}{1 + z^{-m}G(z^{-1})C(z^{-1})} \right\|_\infty < 1. \tag{6}$$

Thus, the constraint of $Q(z^{-1})$ can be easily derived as follows:

$$\|Q(z^{-1})\|_\infty < \left\| \frac{1 + z^{-m}C(z^{-1})G(z^{-1})}{z^{-m}G_m^{-1}(z^{-1})G(z^{-1}) - 1} \right\|_\infty. \tag{7}$$

The magnitude response of $(1 + z^{-m}C(z^{-1})G(z^{-1}))$ is equal to the inverse response of the original sensitivity function and decreases from infinity to one when the frequency increases. $z^{-m}G_m^{-1}(z^{-1})G(z^{-1}) - 1 \approx 0$ is reasonable when $G_m^{-1}(z^{-1}) \approx G(z^{-1})$ in the low- and medial-frequency domains. Thus, it is obvious that (7) is easy to reach if $Q(z^{-1})$ is designed to a low bandwidth less than the frequency in which $G(z^{-1})$ can be modeled accurately. If the plant has uncertainties, which means $\tilde{G}(z^{-1})$ is perturbed equal to $G(z^{-1})(1 + \text{X}(z^{-1}))$. $\text{X}(z^{-1})$ is unknown but has a limited boundary. Substituting $\tilde{G}(z^{-1}) = G(z^{-1})(1+X(z^{-1}))$ into (5), the characteristic polynomial disturbed by the uncertainties X can be derived in the following equation:

$$\begin{aligned} \tilde{P}(z^{-1}) &= 1 + z^{-m}C(z^{-1})G(z^{-1})(1 + X(z^{-1})) \\ &\quad + (z^{-m}G_m^{-1}(z^{-1})(1 + X(z^{-1}))G(z^{-1}) - 1)Q(z^{-1}) \\ &= P(z^{-1})(1 + A(z^{-1})X(z^{-1})). \end{aligned} \tag{8}$$

The stability of (8) is dependent on the stability of $1 + A(z^{-1})X(z^{-1})$, because $P(z^{-1})$ is assumed to be stable according to the above-mentioned analysis. Therefore, (9) can make sure the (8) being stable

$$\|A(z^{-1})X(z^{-1})\|_\infty < 1. \tag{9}$$

Equation (9) implies that the uncertainties $X(z^{-1})$ can be restricted by the original closed-loop transfer function of $A(z^{-1})$ when the control system needs to be stable.

IV. Design of Q-Filter Parameters

According to the aforementioned analysis, ESF(z^{-1}) needs to have a low magnitude at the disturbance frequency of w_i, while $Q(z^{-1}) = 1 - \text{ESF}(z^{-1})$ features a low-pass filter for meeting the closed-loop stability. Considering a simple form of ESF(z^{-1}) as follows:

$$\text{ESF}(z^{-1}) = z^{-2} - 2z^{-1}\cos(w_i) + 1. \tag{10}$$

$Q(z^{-1}) = -z^{-2} + 2z^{-1}\cos(w_i)$ might have an unstable poles of $2\cos(w_i)$ and cannot be implemented in a digital control system, although $\text{ESF}(z^{-1})|_{z=e^{jw_i}} = 0$ implies that it can absolutely eliminate disturbance at the frequency of w_i. In fact, (10) has an equivalent function to eliminate disturbance at the frequency of w_i in comparison with $\text{ESF}(s) = s^2/w_i^2 + 1$ in the frequency domain. We first consider the design procedure in the continuous-time domain and then transform the designed result into that in the discrete-time domain through the bilinear transformation. In fact, $\text{ESF}(s) = s^2/w_i^2 + 1$ is noncausal. Therefore, a proposed notch filter [29] to reduce disturbances is given as follows:

$$\text{ESF}(s) = \frac{\frac{s^2}{w_i^2} + \lambda_i\frac{s}{w_i} + 1}{\frac{s^2}{w_i^2} + \alpha_i\lambda_i\frac{s}{w_i} + 1}. \tag{11}$$

Here, $0 < \lambda_i < 1$ and $\alpha_i > 0$ are designing parameters, which make the performance of the ESF(s) optimal for the tip-tilt mirror control system. The magnitude response

of ESF(s) in frequency domain is derived as follows:

$$|\mathrm{ESF}(jw)|^2 = \frac{\left(1-\frac{w^2}{w_i^2}\right)^2 + \lambda_i^2\frac{w^2}{w_i^2}}{\left(1-\frac{w^2}{w_i^2}\right)^2 + \alpha_i^2\lambda_i^2\frac{w^2}{w_i^2}} \tag{12}$$

where $\alpha_i > 1$ can assure $|\mathrm{ESF}(jw_i)| = 1/a_i < 1$ at the disturbance frequency of w_i such that disturbances could be well mitigated. The differential (12) is derived to know its characteristic

$$\frac{\partial\,|\mathrm{ESF}(jw)|^2}{\partial w} = \frac{2\left(-\alpha_i^2+1\right)\lambda_i^2\frac{w}{w_i^2}\left(1-\frac{w^4}{w_i^4}\right)}{\left[\left(1-\frac{w^2}{w_i^2}\right)^2 + \alpha_i^2\lambda_i^2\frac{w^2}{w_i^2}\right]^2}. \tag{13}$$

From (13), we easily know $(\partial|\mathrm{ESF}(jw)|^2/\partial w) > 0$ when $w > w_i$ and $(\partial|\mathrm{ESF}(jw)|^2/\partial w) < 0$ when $w < w_i$. Furthermore, we have $|\mathrm{ESF}(jw)|_{w\to+\infty} = 1$ and $|\mathrm{ESF}(jw)|_{w\to-\infty} = 1$, arriving at $|\mathrm{ESF}(jw)| \le 1$, which implies this notch filter has a good symmetry. $|\mathrm{ESF}(jw)|$ has a minimum value of $1/a_i$.

Vibration in the frequency domain cannot feature at a single frequency, and usually exhibits a narrowband, which has to be accommodated by ESF(s). Otherwise, it is difficult to be rejected. To know the width of the narrowband, let $h = |\mathrm{ESF}_i(jw)|$, we have

$$h^2 = \frac{\left(1-\frac{w^2}{w_i^2}\right)^2 + \lambda_i^2\frac{w^2}{w_i^2}}{\left(1-\frac{w^2}{w_i^2}\right)^2 + \alpha_i^2\lambda_i^2\frac{w^2}{w_i^2}}. \tag{14}$$

The width Δx of the gap width is easily derived in the following equation:

$$\Delta x = w_i\sqrt{\frac{\lambda_i^2(\alpha_i^2-1)}{1-h^2}}. \tag{15}$$

It is obvious that Δx enlarges as h increases from 0 to 1. This condition of (15) gives a criterion to the design of the parameter λ_i. $Q(s) = 1 - \mathrm{ESF}(s)$ has to feature a low-pass filter such that it can block the unmodeled dynamics and high-frequency noise to affect the closed-loop stability. The following analysis and discussions can verify that $Q(s)$ has a low-filter characteristic. The magnitude response of $Q(jw)$ is derived as follows:

$$|Q(jw)|^2 = \frac{\zeta_i^2(\alpha_i-1)^2\frac{w^2}{w_i^2}}{\left(1-\frac{w^2}{w_i^2}\right)^2 + \alpha_i^2\lambda_i^2\frac{w^2}{w_i^2}}. \tag{16}$$

Fig. 3. Experimental setup of the tip-tilt mirror control system.

In order to obtain the characteristic, the differential of (16) can be derived in the following equation:

$$\frac{|Q(jw)|^2}{\partial w} = \frac{2\left(\alpha_i-1\right)^2\lambda_i^2\frac{w}{w_i^2}\left(1-\frac{w^2}{w_i^2}\right)\left(1+\frac{w^2}{w_i^2}\right)}{\left[\left(1-\frac{w^2}{w_i^2}\right)^2 + \alpha_i^2\lambda_i^2\frac{w^2}{w_i^2}\right]^2}. \tag{17}$$

In comparison with (13), $|Q(jw)|^2/\partial w$ has a similarity to $|\mathrm{ESF}(jw)|^2/\partial w$. Therefore, the magnitude of $|Q(jw)|^2$ increases monotonously as the frequency increases when the $w < w_i$, while the function of $|Q(jw)|^2$ decreases monotonously as the frequency decreases when $w < w_i$. $|Q(jw)|$ has a maximum magnitude response close to $(1 - 1/\alpha_i) \le 1$ when $w = w_i$. Thus, $Q(s)$ is a bandpass filter, and of course, characterizes a low-pass filter. A multiplicity of (11) is used to reject numbers of narrowband vibrations shown in (18) and (19), as shown at the bottom of this page.

Supposed that the disturbance $D_i(s)$ has a magnitude A_i responding to the frequency of w_i. Combining with (19), the disturbance can be arrived to $M\_\mathrm{EFS}(s)\sum_{i=1}^{k} D_i(s) \approx \sum_{i=1}^{k} A_i/\alpha_i$. Using the bilinear transformation, the transfer function of (18), is expressed in (19) in z-domain, where T is the sampling time.

V. Experimental Setup and Validation

To verify the proposed method being effective, a simplified experimental setup of the tip-tilt mirror control system is built in Fig. 3, and mainly includes image process units, light source, tip-tilt mirror, and control processing unit. The disturbance mirror is also a tip-tilt mirror with a high control

$$M\_\mathrm{ESF}(s) = \prod_{i=1}^{k}\frac{\frac{s^2}{w_i^2} + \lambda_i\frac{s}{w_i} + 1}{\frac{s^2}{w_i^2} + \alpha_i\lambda_i\frac{s}{w_i} + 1} \tag{18}$$

$$M\_\mathrm{ESF}(z^{-1}) = \prod_{i=1}^{k}\frac{\left(\frac{4}{w_i^2} + T^2 - \frac{2T\varsigma_i}{w_i}\right)z^{-2} + \left(-\frac{8}{w_i^2} + 2T^2\right)z^{-1} + \frac{4}{w_i^2} + T^2 + \frac{2T\lambda_i}{w_i}}{\left(\frac{4}{w_i^2} + T^2 - \alpha_i\frac{2T\lambda_i}{w_i}\right)z^{-2} + \left(-\frac{8}{w_i^2} + 2T^2\right)z^{-1} + \frac{4}{w_i^2} + T^2 + \alpha_i\frac{2T\lambda_i}{w_i}} \tag{19}$$

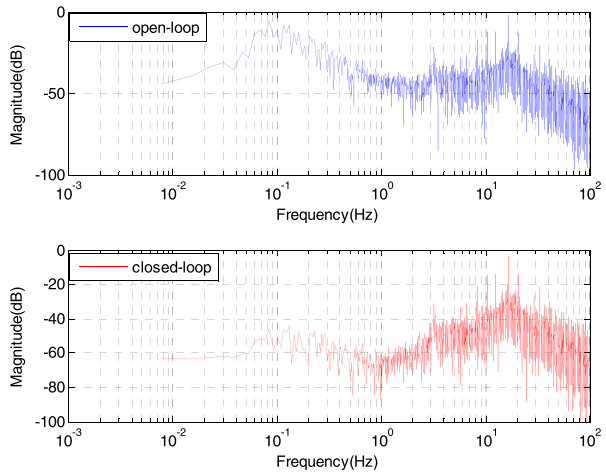

Fig. 4. Open-loop and closed-loop spectra of tip-tilt vibrations.

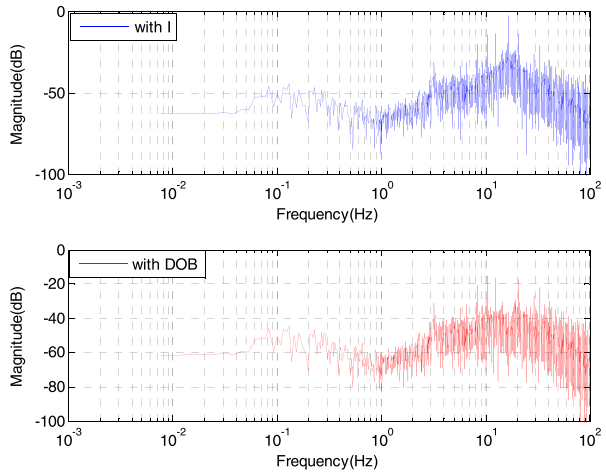

Fig. 5. Spectra of tip-tilt vibrations with I and DOB.

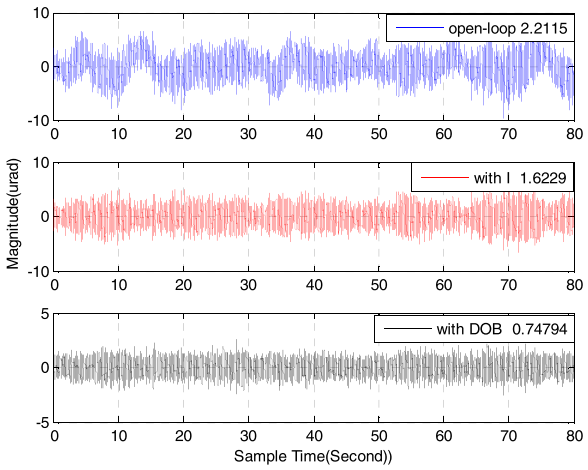

Fig. 6. Tip-tilt errors with the open loop, integral, and DOB.

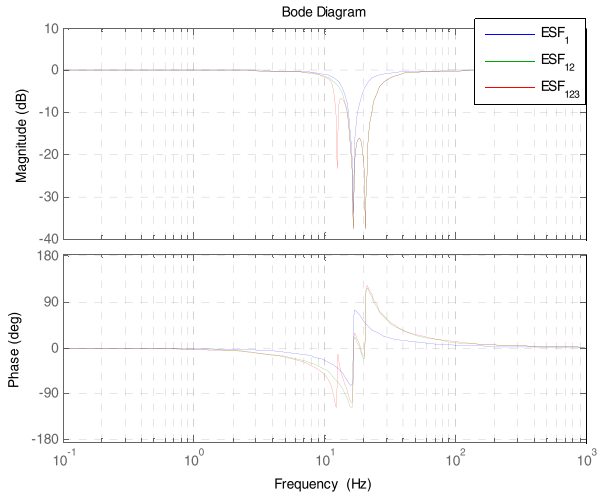

Fig. 7. Bode responses with different ESF(s).

bandwidth and is used to simulate vibrations, which can be detected by the image sensor. The high precision line-of-sight error (position error) is obtained through the centroiding algorithm. The image sensor (charged-coupled device) updates in 200 Hz. The tip-tilt mirror has a stroke of $+/-1$ mard and a closed-loop resolution of less than 0.5-urad rms. Due to the high-rate sampling eddy sensor to measure the angular position of the tip-tilt mirror, the control bandwidth of this tip-tilt mirror is more than 500 Hz.

The spectra of vibrations in tip-tilt mode are shown in Fig. 4. The blue line represents the spectra in open-loop mode, while the red line exhibits the spectra of the closed-loop tip-tilt error when the controller is an integrator. It is shown that energetic vibrations mainly focus on the frequencies between 10 and 20 Hz. The vibration in the frequency of about 17-Hz features high magnitude and narrowband. It is obvious that this vibration cannot be well rejected by a limited bandwidth loop.

Fig. 5 compares the spectra of the tip-tilt errors when the control system is used integrator (I) and the improved DOB. The magnitude response with the integral controller is depicted in the blue line. Vibrations between 10 and 20 Hz are obvious not to be rejected. To mitigate them, the improved DOB controller shown in Fig. 2(b) is executed. Due to a notch filter with the basic frequency of about 17 Hz being brought into the control system, high rejection at the energetic frequencies is provided, leading to a big reduction in this area, although the DOB introduces a little amplification at other frequencies.

Fig. 6 compares errors in different situations. It is shown that the tip-tilt vibrations with the DOB can arrive at 0.75-urad rms, less than 46.1% of that with the originally integral controller. However, two kinds of narrowband vibrations still occur at the frequencies of 13 and 21 Hz. Only one notch filter employing in the DOB cannot give a better result in Fig. 6. Using (19) to produce multiple notch filters, the other two kinds of notch filters are designed to reject disturbances at the other frequencies besides the basic frequency of 17 Hz.

The magnitude responses of different extra sensitivity functions are demonstrated in Fig. 7. ESF_1 used in Fig. 6 only incorporates a notch filter with the centered frequency of 17 Hz. ESF_{12} is added with another notch filter with the centered frequency of 21 Hz in comparison with ESF_1. ESF_{123} includes three notch filters, which can cope with three-band vibrations.

The resulting errors with different Q-filters in the time domain are demonstrated in Fig. 8. Because three peak vibrations can be mitigated by ESF_{123}, which leads to the best

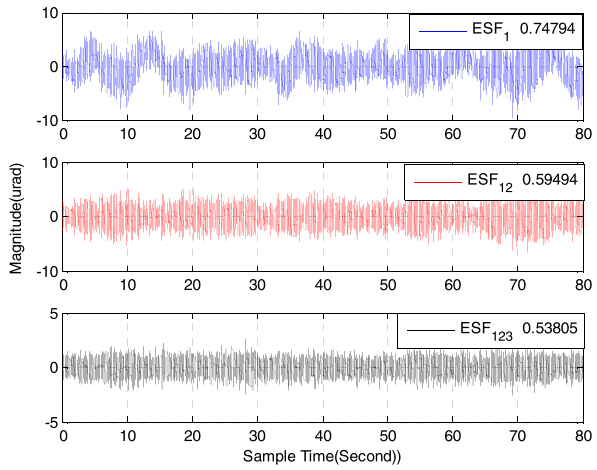

Fig. 8. Tip-tilt vibrations with different ESF(s) in the time domain.

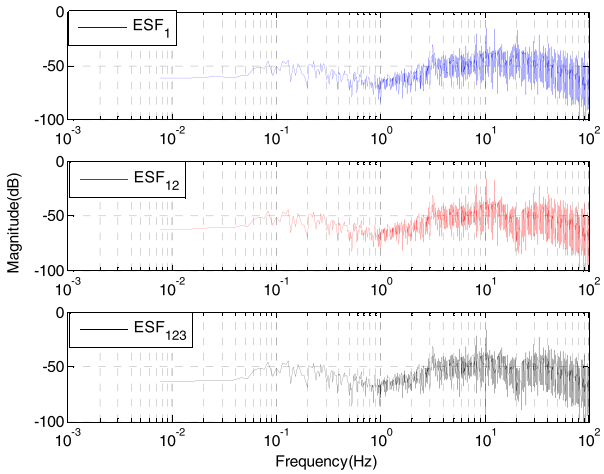

Fig. 9. Spectra of tip-tilt vibrations with different ESF(s).

results with 0.54-urad rms, less than 33.1% of that with the only feedback integral controller.

The spectra of the resulting errors are shown in Fig. 9, responding to different ESF(s) shown in Fig. 8. Although numbers of notch filters are increased, leading to a better improvement on the control performance, phase loss induced by these filters could deteriorate the control stability, and evenly destroys it. Amplifications induced by any of extra sensitivity functions at other frequencies are almost not seen in Fig. 9, which implies that the waterbed effect induced by this controller is small.

VI. Conclusion

In this paper, a new controller based on DOB of the tip-tilt mirror to mitigate mechanical vibrations of the astronomical telescope has been proposed and experimentally verified. We give detailed introductions of the design process of the DOB control system, the optimization of the control, and Q-filter parameters. The closed-loop bandwidth is not widened with this proposed DOB control mode but the disturbance attenuation is improved. The use of this new controller is not confined to the tip-tilt mirror control system but also can be extended to the other servo control system with only position error available because of its simple structure and design process. The improved DOB controller depends on a simple Q-filter and a low-frequency plant model such that disturbance rejection at expected frequencies can be easily arrived. An improved bandpass filter is investigated to mitigate multiple narrowband vibrations and also to avoid big amplifications at other frequencies. In this DOB control mode, disturbances can be attenuated less than 1/3 of the conventional feedback control level in the tip-tilt mirror control system. Next work will focus on disturbance rejections beyond the Nyquist frequency, and the estimation of disturbance frequencies and the control model online. Taylor weighted least squares algorithm could be used to estimate disturbance frequencies [32].

Acknowledgment

The authors would like to thank T. Yang and C. Fu for their kind help with the experimental work.

References

[1] J. R. Maly, D. Erickson, and T. J. Pargett, "Vibration suppression for the Gemini Planet Imager," *Proc. SPIE*, vol. 7733, pp. 77331F-1–77331F-9, Jul. 2010.

[2] C. Kulcsár *et al.*, "Vibrations in AO control: A short analysis of on-sky data around the world," *Proc. SPIE*, vol. 8447, pp. 84471C-1–84471C-14, Sep. 2012.

[3] S. Zúñiga *et al.*, "Vibrations in MagAO: Frequency-based analysis of on-sky data, resonance sources identification, and future challenges in vibrations mitigation," *Proc. SPIE*, vol. 9909, pp. 99093L-1–99093L-6, Jul. 2016.

[4] L. G. Sivo *et al.*, "First on-sky SCAO validation of full LQG control with vibration mitigation on the CANARY pathfinder," *Opt. Express*, vol. 22, no. 19, pp. 23565–23591, 2014.

[5] C. Correia, J.-P. Véran, and G. Herriot, "Advanced vibration suppression algorithms in adaptive optics systems," *J. Opt. Soc. Amer. A, Opt. Image Sci.*, vol. 29, no. 3, pp. 185–194, 2012.

[6] G. Sivo, "Full LQG control with vibration mitigation: From theory to first on-sky validation on the CANARY MOAO demonstrator," in *Imag. Appl. Opt., OSA Tech. Dig.*, 2013, Paper OTu2A.2.

[7] S. Meimon, C. Petit, T. Fusco, and C. Kulcsár, "Tip–tilt disturbance model identification for Kalman-based control scheme: Application to XAO and ELT systems," *J. Opt. Soc. Amer. A, Opt. Image Sci.*, vol. 27, no. 11, pp. A122–A132, 2010.

[8] A. Keck, J. Pott, T. Ruppel, and O. Sawodny, "Development of new concepts to minimize the impact of fast telescope vibrations seen by the E-ELT/MICADO wavefront sensors," *Proc. SPIE*, vol. 8447, pp. 84474W-1–84474W-8, Sep. 2012.

[9] C. Petit, J. M. Conan, C. Kulcsár, H.-F. Raynaud, and T. Fusco, "First laboratory validation of vibration filtering with LQG control law for Adaptive Optics," *Opt. Express*, vol. 16, no. 1, pp. 87–97, 2008, doi: 10.1364/OE.16.000087.

[10] Y. Clenet, M. E. Kasper, and T. Fusco, "NACO performance: Status after 2 years of operation," *Proc. SPIE*, vol. 5490, pp. 107–117, Oct. 2004.

[11] M. Böhm, J.-U. Pott, M. Kürster, and O. Sawodny, "Modeling and identification of the optical path at ELTs—A case study at the LBT," *IFAC Proc. Vol.*, vol. 46, no. 5, pp. 249–255, Apr. 2013.

[12] M. Castro *et al.*, "Closed-loop control for tip-tilt compensation on systems under vibration," *Proc. SPIE*, vol. 9909, pp. 99093K-1–99093K-6, Jul. 2016.

[13] A. Keck, J.-U. Pott, and O. Sawodny, "Accelerometer-based online reconstruction of vibrations in extremely large telescopes," *IFAC Proc. Vol.*, vol. 47, no. 3, pp. 7467–7473, 2014.

[14] M. Böhm, J.-U. Pott, M. Kürster, O. Sawodny, D. Defrère, and P. Hinz, "Delay compensation for real time disturbance estimation at extremely large telescopes," *IEEE Trans. Control Syst. Technol.*, vol. 25, no. 4, pp. 1384–1393, Jul. 2017.

[15] M. Glück, J.-U. Pott, and O. Sawodny, "Piezo-actuated vibration disturbance mirror for investigating accelerometer-based tip-tilt reconstruction in large telescopes," *IFAC-PapersOnLine*, vol. 49, no. 21, pp. 361–366, 2016.

[16] C. Petit, J.-M. Conan, C. Kulcsár, and H.-F. Raynaud, "Linear quadratic Gaussian control for adaptive optics and multiconjugate adaptive optics: Experimental and numerical analysis," *J. Opt. Soc. Amer. A, Opt. Image Sci.*, vol. 26, no. 6, pp. 1307–1325, 2009.

[17] G. Agapito, F. Quirós-Pacheco, P. Tesi, A. Riccardi, and S. Esposito, "Observer-based control techniques for the LBT adaptive optics under telescope vibrations," *Eur. J. Control*, vol. 17, no. 3, pp. 316–326, 2011.

[18] A. Guesalaga, B. Neichel, J. O'Neal, and D. Guzman, "Mitigation of vibrations in adaptive optics by minimization of closed-loop residuals," *Opt. Express*, vol. 21, no. 9, pp. 10676–10696, 2013.

[19] C. J. Kempf and S. Kobayashi, "Disturbance observer and feedforward design for a high-speed direct-drive positioning table," *IEEE Trans. Control Syst. Technol.*, vol. 7, no. 5, pp. 513–526, Sep. 1999.

[20] M. Zheng, S. Zhou, and M. Tomizuka, "A design methodology for disturbance observer with application to precision motion control: An H-infinity based approach," in *Proc. Amer. Control Conf. (ACC)*, Seattle, WA, USA, May 2017, pp. 3524–3529.

[21] J. Yang, S. Li, and X. Yu, "Sliding-mode control for systems with mismatched uncertainties via a disturbance observer," *IEEE Trans. Ind. Electron.*, vol. 60, no. 1, pp. 160–169, Jan. 2013.

[22] M. Tomizuka, "Controller structure for robust high-speed/high accuracy digital motion control," in *Proc. IEEE Conf. Robot. Automat. Notes Tutorial Session*, 1994.

[23] B. Yao, M. Al-Majed, and M. Tomizuka, "High performance robust motion control of machine tools: An adaptive robust control approach and comparative experiments," in *Proc. Amer. Control Conf.*, Jun. 1997, pp. 2754–2758.

[24] B. K. Kim and W. K. Chung, "Advanced disturbance observer design for mechanical positioning systems," *IEEE Trans. Ind. Electron.*, vol. 50, no. 6, pp. 1207–1216, Dec. 2003.

[25] X. Wei and L. Guo, "Composite disturbance-observer-based control and H_∞ control for complex continuous models," *Int. J. Robust Nonlinear Control*, vol. 20, no. 1, pp. 106–118, 2010.

[26] L. Besnard, Y. B. Shtessel, and B. Landrum, "Quadrotor vehicle control via sliding mode controller driven by sliding mode disturbance observer," *J. Franklin Inst.*, vol. 349, no. 2, pp. 658–684, 2012.

[27] A. Kakami, T. Muto, Y. Yano, and T. Tachibana, "A method for evaluating the thrust of a space propulsion device with wide range time variations using a disturbance observer," *Rev. Sci. Instrum.*, vol. 86, no. 11, p. 115114, 2015.

[28] S. Dasgupta, S. Sadhu, and T. K. Ghoshal, "Designing disturbance observer for non-linear systems—A Hirschorn inverse approach," *IET Sci., Meas. Technol.*, vol. 11, no. 2, pp. 164–170, 2017.

[29] T. Tang, B. Qi, and T. Yang, "Youla–Kucera parameterization-based optimally closed-loop control for tip–tilt compensation," *IEEE Sensors J.*, vol. 18, no. 15, pp. 6154–6160, Aug. 2018.

[30] M. Loueipour, M. Keshmiri, M. Danesh, and M. Mojiri, "Wave filtering and state estimation in dynamic positioning of marine vessels using position measurement," *IEEE Trans. Instrum. Meas.*, vol. 64, no. 12, pp. 3253–3261, Dec. 2015.

[31] X. Chen and M. Tomizuka, "Optimal decoupled disturbance observers for dual-input single-output systems," *ASME J. Dyn. Syst., Meas., Control*, vol. 136, no. 5, p. 051018, 2014.

[32] D. Belega, D. Fontanelli, and D. Petri, "Dynamic phasor and frequency measurements by an improved Taylor weighted least squares algorithm," *IEEE Trans. Instrum. Meas.*, vol. 64, no. 8, pp. 2165–2178, Aug. 2015.

Tao Tang (M'18) received the Ph.D. degree in mechanical engineering from the University of the Chinese Academy of Sciences, Beijing, China, in 2009.

From 2014 to 2016, he was a Visiting Scholar with the University of California at Berkeley, Berkeley, CA, USA. He is currently an Associate Professor with the Institute of Optics and Electronics, Chinese Academy of Sciences, Beijing. His current research interests include basic theory and engineering applications in optoelectronic engineering, especially inertial stabilization technology, vibration rejections, and image-based visual servoing system.

Shuaixu Niu was born in Handan, Hebei, China. She received the bachelor's degree from the Tangshan College, Tangshan, China, in 2012. She is currently pursuing the Ph.D. degree with the University of Chinese Academy of Sciences, Beijing, China, with a focus on the vibration rejections of tip-tilt mirror.

Xiaoqiang Chen received the bachelor's degree from Yangzhou University, Yangzhou, China, in 2003.

He is currently a Senior Engineer with the Institute of Aerospace System Engineering, Shanghai, China. His current research interests include computer science and the architecture design of the electronic system.

Bo Qi received the Ph.D. degree in optical engineering from the University of the Chinese Academy of Sciences, Beijing, China, in 2012.

He is currently a Professor with the Institute of Optics and Electronics, Chinese Academy of Sciences, Beijing. His current research interests include optical structure design, optical engineering, beam control technology, laser communication, quantum communication, space camera, and optical precision tracking and measurement.